Method for Computing Component Fugacities of Binary Mixtures in Vapor-Liquid Equilibrium with Results for Methane–Propane, Methane–*n*-Butane, and Methane–*n*-Pentane

James W. Leach[1]
LTV Aerospace Corp., Dallas, Tex. 75222

A method for computing the fugacities of components of binary mixtures at conditions of vapor-liquid equilibrium is presented. The new method utilizes coexisting phase composition and volumetric data rather than gas-phase partial volumetric data in the computations of the component fugacities. This permits an improvement in the accuracy of the computed results and increases the range of pressures for which computations can be made at isothermal vapor-liquid equilibrium conditions. Coexisting phase data published in the literature are analyzed to obtain results for methane–propane, methane–*n*-butane, and methane–*n*-pentane. Fugacity computations based on a limited quantity of gas-phase partial volumetric data are made to check the results obtained by the new method.

Component fugacity data of mixtures at conditions of vapor-liquid equilibrium have practical and theoretical importance. Coexisting phase property data are required for the design of separation units in the production and refining of petroleum. In addition, component fugacity data may be used to evaluate and develop theories (*5*) for computing liquid and vapor compositions and thermodynamic properties which must be able to predict the component fugacities to establish conditions of equilibrium.

A method for computing the fugacities of the components of a binary mixture at conditions of vapor-liquid equilibrium is presented. This method utilizes coexisting phase composition and volumetric data to minimize the effects of experimental errors on the computations.

The data of Sage and Lacey (*8*) are analyzed to obtain results for methane–propane, methane–*n*-butane, and methane–*n*-pentane.

Analysis

If the fugacities of the components of a mixture are known at a reference state, and sufficient experimental data exist for the mixture, the fugacities of the components at the mixture conditions can be determined by integrating the total derivatives of the fugacities from the known conditions to the mixture conditions. For a binary mixture at the temperature of the reference state,

$$\ln f_i = \ln f_1^0 + \int_{P^0}^{P} \left(\frac{\partial \ln f_i}{\partial P}\right)_{T,N_1,N_2} dP + \int_{N_1^0}^{N_1} \left(\frac{\partial \ln f_i}{\partial N_1}\right)_{T,P,N_2} dN_1 + \int_{N_2^0}^{N_2} \left(\frac{\partial \ln f_i}{\partial N_2}\right)_{T,P,N_1} dN_2 \quad (1)$$

Equation 1 expresses the change in a property of the mixture in terms of a complete set of independent variables. Since N_1, N_2, and P can always be varied independently, Equation 1 is applicable to single or two-phase systems. Theoretically, the value of the fugacity computed from Equation 1 is independent of the integration path. However, because of experimental errors in the mixture data, it is desirable to choose the path of integration so as to maximize the accuracy of the results. Typically (*4*), the integration is performed over a path such as *A–B* shown in Figure 1. The fugacity at state *A* in Figure 1 can be evaluated from ideal gas relationships. For path *A–B* the mole fractions are constant so that Equation 1 becomes

$$\int_A^B d(\ln f_i) = \int_{P_A}^{P_B} \left(\frac{\partial \ln f_i}{\partial P}\right)_{T,N_1N_2} dP = \frac{1}{RT}\int_{P_A}^{P_B} \bar{V}_i dP \quad (2)$$

To compute the partial volume $\bar{V}_i$ in Equation 2, one must mathematically differentiate the relationship between the mixture volume and the mixture composition. Therefore, small experimental errors in the volumetric data along path *A–B* can cause large errors in the computations of the partial volumes and in the fugacity calculations. Also, fugacities cannot be calculated in the retrograde condensate region from gas-phase partial volumetric data alone.

In this work the component fugacities are evaluated by integrating over paths such as *C–D* shown in Figure 1. This eliminates the requirements for gas-phase partial volumetric data and provides a means for computing fugacities in the coexisting phase region between the liquid and retrograde condensate.

The component fugacities are constant along segments such as 1–2 on path *C–D*. Therefore, for path *C–D*, two of the terms in Equation 1 are identically zero.

$$\int_{N_i}^{N_1} \left(\frac{\partial \ln f_i}{\partial N_1}\right)_{T,P,N_2} dN_1 = \int_{N_2^0}^{N_2} \left(\frac{\partial \ln f_i}{\partial N_2}\right)_{T,P,N_1} dN_2 = 0 \quad (3)$$

Thus, changes in the component fugacities are given by:

$$\Delta(\ln f_i) = \int_{P}^{P+\Delta P} \left(\frac{\partial \ln f_i}{\partial P}\right)_{T,N_1,N_2} dP \quad (4)$$

The integrand in Equation 4 may be replaced (*10*) by

$$\left(\frac{\partial (\ln f_i)}{\partial P}\right)_{T,N_1,N_2} = \frac{1}{RT}\left(\frac{\partial V}{\partial N_i}\right)_{T,P,N_{j\neq i}} \quad (5)$$

Equations 4 and 5 require expressions for the partial derivatives of the mixture volume with respect to the number of moles of each constituent in the coexisting phase region. In this region the mixture volume is the sum of the volumes occupied by the liquid and vapor phases. The mole fractions in each phase are dependent only on temperature and pressure, but the number of moles in each phase changes with the mixture composi-

[1] Research initiated at Rice University, Houston, Tex.

tion at constant temperature and pressure. Therefore, for the coexisting phase region,

$$\left(\frac{\partial V}{\partial N_1}\right)_{T,P,N_2} = v_f \left(\frac{\partial N_f}{\partial N_1}\right)_{T,P,N_2} + v_g \left(\frac{\partial N_g}{\partial N_1}\right)_{T,P,N_2} \quad (6)$$

Equations for $(\partial N_f/\partial N_1)_{T,P,N(2)}$ and $(\partial N_g/\partial N_1)_{T,P,N(2)}$ can be obtained from:

$$\left(\frac{\partial N_1}{\partial N_1}\right)_{T,P,N_2} = \left(\frac{\partial N_{1g}}{\partial N_1}\right)_{T,P,N_2} + \left(\frac{\partial N_{1f}}{\partial N_1}\right)_{T,P,N_2} = 1 \quad (7)$$

$$\left(\frac{\partial N_2}{\partial N_1}\right)_{T,P,N_2} = \left(\frac{\partial N_{2g}}{\partial N_1}\right)_{T,P,N_2} + \left(\frac{\partial N_{2f}}{\partial N_1}\right)_{T,P,N_2} = 0 \quad (8)$$

$$\left(\frac{\partial x_1}{\partial N_1}\right)_{T,P,N_2} = \frac{\partial}{\partial N_1}\left(\frac{N_{1f}}{N_{1f}+N_{2f}}\right)_{T,P,N_2} = 0 \quad (9)$$

$$\left(\frac{\partial y_1}{\partial N_1}\right)_{T,P,N_2} = \frac{\partial}{\partial N_1}\left(\frac{N_{1g}}{N_{1g}+N_{2g}}\right)_{T,P,N_2} = 0 \quad (10)$$

The results are:

$$\left(\frac{\partial N_f}{\partial N_1}\right)_{T,P,N_2} = \frac{y_2}{x_1 - y_1} \quad (11)$$

$$\left(\frac{\partial N_g}{\partial N_1}\right)_{T,P,N_2} = \frac{-x_2}{x_1 - y_1} \quad (12)$$

With these results Equation 6 becomes:

$$\left(\frac{\partial V}{\partial N_1}\right)_{T,P,N_2} = \frac{y_2 v_f - x_2 v_g}{x_1 - y_1} \quad (13)$$

An expression for $(\partial V/\partial N_2)_{T,P,N(1)}$ is obtained by exchanging indices.

$$\left(\frac{\partial V}{\partial N_2}\right)_{T,P,N_1} = \frac{y_1 v_f - x_1 v_g}{x_2 - y_2} \quad (14)$$

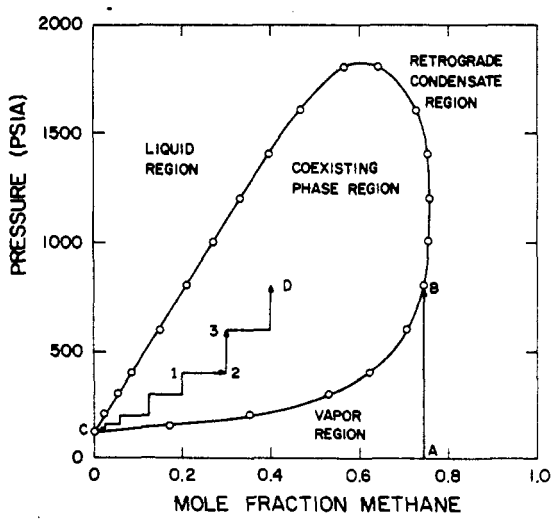

Figure 1. Isothermal pressure composition diagram for methane–*n*-butane at 160°F

Equations 13 and 14 may be used to compute the quantities in the integrals for $\Delta(\ln f_1)$ and $\Delta(\ln f_2)$ from data for the saturated liquid and saturated vapor at points along the integration path. Changes in the component fugacities can then be obtained by evaluating the integrals numerically.

A singularity exists in $(\partial V/\partial N_1)_{T,P,N(2)}$ at $x_1 = 0$ which causes some difficulty in evaluating $\Delta(\ln f_1)$ at pressures near the saturation pressure of the heavier component. However, the product

$$\frac{(P - P_g)}{RT}\left(\frac{\partial V}{\partial N_1}\right)_{T,P,N_2}$$

is nearly constant when plotted vs. pressure, so that changes in the fugacity of methane are easily determined at higher pressures. Some typical values of $(\partial V/\partial N_2)_{T,P,N(1)}$ and $[(P - P_g)/RT](\partial V/\partial N_1)_{T,P,N(2)}$ computed from data for the methane–*n*-butane system at 100°F are shown in Figure 2. Figure 2 shows that these quantities may be approximated by linear functions of pressure to evaluate small changes in the component fugacities.

$$\left(\frac{\partial V}{\partial N_1}\right)_{T,P,N_2} = \frac{a_1 + b_1 P}{P - P_g} \quad (15)$$

$$\left(\frac{\partial V}{\partial N_2}\right)_{T,P,N} = a_2 + b_2 P \quad (16)$$

With these approximations the equations for $d(\ln f_i)$ may be integrated for small changes in pressure.

$$RT\Delta(\ln f_1) = (a_1 + b_1 P_g) \cdot \log\left[1 + \left(\frac{\Delta P}{P - P_g}\right)\right] + b_1 \Delta P \quad (17)$$

$$RT\Delta(\ln f_2) = a_2 \Delta P + b_2\left(P\Delta P + \frac{\Delta P^2}{2}\right) \quad (18)$$

Equations 17 and 18 were used to compute changes in the component fugacities between successive data points on path *C–D*. The coefficients a_1, b_1, a_2, and b_2 were evaluated from the coexisting phase data at the beginning and the end of each segment of the integration path.

Absolute values of the component fugacities depend on the fugacities at some reference state. The fugacity of the heavier hydrocarbon in each system was evaluated at $x_1 = 0$ from pure component compressibility data for propane, *n*-butane, and *n*-pentane (*1–3, 6–8*). Although the fugacity of methane is zero at $x_1 = 0$, this condition can-

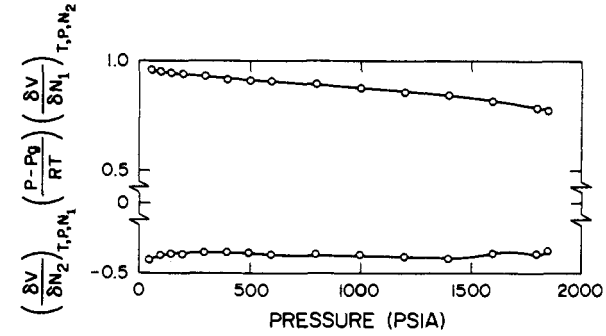

Figure 2. Quantities in integrands of $\Delta(\ln f_1)$ and $\Delta(\ln f_2)$ for methane–*n*-butane at 100°F

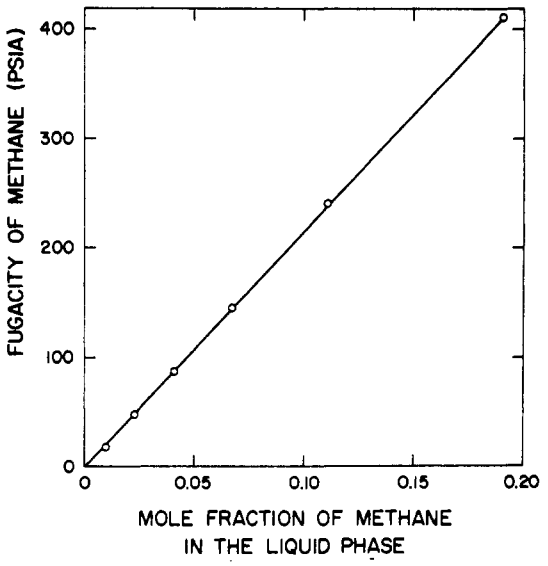

Figure 3. Fugacity of methane at saturation conditions in methane–propane system at 100°F

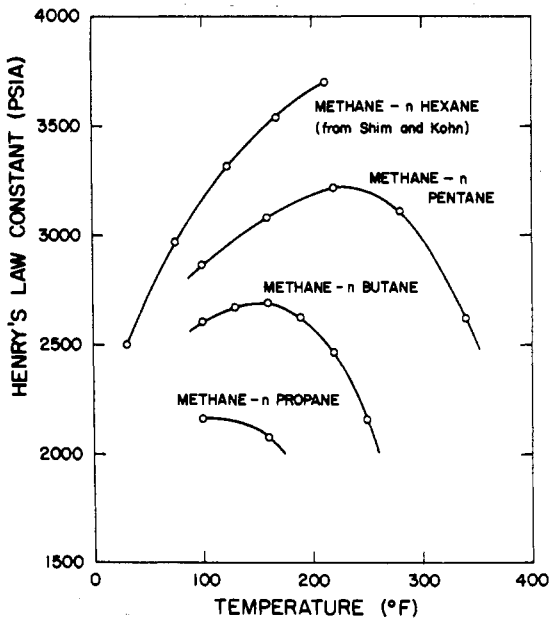

Figure 4. Henry's Law constant for methane

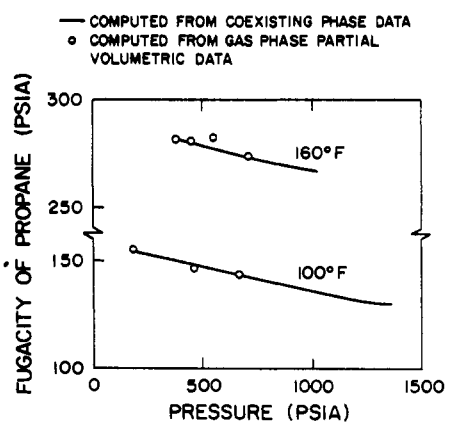

Figure 5. Fugacity of propane at saturation conditions in methane–propane system

not be used as a reference state because of the singularity in $(\partial V/\partial N_1)_{T,P,N(2)}$. To obtain the fugacity of methane at a reference state in the coexisting phase away from the singularity, the mixture fugacity at dew-point conditions was computed by integrating along paths such as *A–B* in Figure 1.

$$\ln\left(\frac{f}{P}\right)_B = \int_0^{P_B}\left(\frac{Z-1}{P}\right)dP \qquad (19)$$

The integral in Equation 19 was evaluated with the following equation of state:

$$Z = 1 + aP + bP^2 \qquad (20)$$

Integration from point "*A*" to the data point on path *A–B* with the lowest pressure was accomplished with the coefficient "*a*" in Equation 20 determined from second virial coefficient data, and "*b*" from compressibility data at the first data point. At higher pressures both coefficients in Equation 20 were determined from compressibility data at consecutive points on the integration path. Equation 19 does not require partial volumetric data for the gas phase since the component fugacities are not computed.

The fugacity of methane in the saturated vapor at *B* was determined from the mixture fugacity given by Equation 19, and the fugacity of the heavier component given by Equation 18, by the following equation:

$$y_1 \ln\left(\frac{f_1}{y_1 P}\right)_B = \ln\,(f/P)_B - y_2 \ln\left(\frac{f_2}{y_2 P}\right)_B \qquad (21)$$

Some typical values of the fugacity of methane computed from Equation 21 are shown in Figure 3. This figure shows a linear relationship between fugacity and mole fraction, in accordance with Henry's Law. This linear relationship was used to smooth the fugacities computed from Equation 21 and establish reference states for methane in the coexisting phase region for each isotherm. The reference states established for methane for the three systems studied in this work are indicated in Tables I–III. These states are near the maximum compo-

Table I. Coexisting Phase Fugacities for Methane–Propane System

100°F			160°F		
Press, psia	Fugacity, psia, propane	Methane	Press, psia	Fugacity, psia, propane	Methane
189[a]	154.7[b]	0	384[a]	282.3[b]	0
200	154.5	11.6	400	281.8	13.1
250	153.5	55.5	450	280.3	51.5
300	152.4	99.5	500	278.9	90
350	151.3	141	550	277.7	130
400	150.2	183	600	276.4	169[c]
450	149.0	225[c]	650	275.2	206
500	147.8	266	700	274.1	242
600	145.5	347	750	272.9	277
700	143.1	426	800	271.9	312
800	140.8	503	850	270.9	345
900	138.6	578	900	270.0	377
1000	136.4	651	950	269.1	408
1100	134.2	721	1000	268.0	440
1200	132.1	789	1020	267.4	453
1300	130.2	854			
1353[d]	129.3	886			

[a]Vapor pressure of propane. [b]Reference fugacity of propane. [c]Reference fugacity of methane. [d]Critical pressure.

Table II. Coexisting Phase Fugacities for Methane–*n*-Butane System

100°F			130°F			160°F		
Press, psia	Fugacity, psia, *n*-butane	Methane	Press, psia	Fugacity, psia, *n*-butane	Methane	Press, psia	Fugacity, psia, *n*-butane	Methane
51.5[a]	46.9[b]	0	80.6[a]	71.1[b]	0	120.6[a]	102.6[b]	0
100	46.8	45.8	100	71.1	17.1	150	102.6	24
200	46.4	138[c]	200	70.8	107	200	102.5	65
300	46.1	224	300	70.4	196[c]	300	102.3	154[c]
400	45.8	306	400	70.1	276	400	102.0	230
500	45.5	386	500	69.8	354	500	101.7	303
600	45.2	464	600	69.4	430	600	101.5	374
800	44.6	614	800	68.8	576	800	100.9	510
1000	44.0	756	1000	68.2	716	1000	100.2	642
1200	43.3	893	1200	67.5	850	1200	99.6	769
1400	42.7	1023	1400	66.9	978	1400	99.1	891
1600	42.1	1148	1600	66.3	1102	1600	98.5	1009
1800	41.6	1266	1800	65.7	1220	1800	98.1	1123
1912[d]	41.3	1328	1876[d]	65.5	1264	1810[d]	98.1	1128
	190°F			220°F			250°F	
174.4[a]	142.4[b]	0	241.2[a]	188.2[b]	0	327.7[a]	242.7[b]	0
200	142.4	17	300	188.5	43	400	243.9	47
300	142.4	102	400	189.0	118	500	245.4	114
400	142.3	183[c]	500	189.4	193[c]	600	246.8	184[c]
500	142.3	252	600	189.7	255	800	249.1	285
600	142.2	319	800	190.0	373	1000	250.8	383
800	141.9	447	1000	189.9	489	1200	251.6	431
1000	141.5	571	1200	189.7	602	1264[d]	253.3	506
1200	141.0	692	1400	189.4	712			
1400	140.4	810	1520[d]	189.2	777			
1600	139.6	926						
1698[d]	139.2	982						

[a]Vapor pressure of *n*-butane. [b]Reference fugacity of *n*-butane. [c]Reference fugacity of methane. [d]Critical pressure.

Table III. Coexisting Phase Fugacities for Methane–*n*-Pentane System

100°F			160°F			220°F		
Press, psia	Fugacity, psia, *n*-pentane	Methane	Press, psia	Fugacity, psia, *n*-pentane	Methane	Press, psia	Fugacity, psia, *n*-pentane	Methane
15.69[a]	14.99[b]	0	42.48[a]	38.83[b]	0	94.91[a]	81.66[b]	0
100	14.95	82.5	100	38.86	55	100	81.67	5
200	14.91	179.1	200	38.87	148[c]	200	81.86	97
300	14.86	274	300	38.87	239	300	81.99	190
400	14.82	367	400	38.86	239	400	82.10	279[c]
600	14.74	547	600	38.83	507	600	82.24	456
800	14.67	719	800	38.79	680	800	82.33	630
1000	14.62	883	1000	38.77	847	1000	82.43	801
1250	14.58	1078	1250	38.80	1049	1250	82.68	1008
1500	14.58	1263	1500	38.90	1242	1500	83.07	1208
1750	14.61	1438	1750	39.07	1428	1750	83.41	1404
2000	14.67	1603	2000	39.26	1607	2000	83.93	1594
2250	14.74	1759	2250	39.46	2000	2081[d]	84.22	1653
2455[d]	14.79	1881	2338[d]	39.54	1838			
	280°F			340°F				
185.55[a]	147.6[b]	0	329.16[a]	238.7[b]	0			
200	147.7	13	400	239.0	50			
300	148.0	105	600	240.2	217[c]			
400	148.3	192	800	241.4	371			
600	148.7	366[c]	1000	242.0	526			
800	149.3	537	1025[d]	242.0	546			
1000	149.9	704						
1250	150.6	909						
1500	151.1	1111						
1610[d]	151.3	1200						

[a]Vapor pressure of *n*-pentane. [b]Reference fugacity of *n*-pentane. [c]Reference fugacity of methane. [d]Critical pressure.

sition of methane for which Henry's Law is applicable. The Henry's Law constants computed for each of the systems studied in this work are shown in Figure 4. Values reported by Shim and Kohn (*9*) for the methane–*n*-hexane system are also shown in Figure 4.

To check the results of this work, the component fugacities were computed from partial volumetric data for the gas phase (*8*) and from second virial coefficient data (*1–3, 6, 7*). Integration of Equation 2 from $P = 0$ to P gives:

$$\ln\left(\frac{f_i}{y_i P}\right) = \int_0^P \left(\frac{P\bar{V}_i}{RT} - 1\right)\frac{dP}{P} \qquad (22)$$

The integrand in Equation 22 was approximated by linear functions of pressure to evaluate changes in the component fugacities between consecutive data points on path *A–B* in Figure 1.

$$\left(\frac{P\bar{V}_i}{RT}\right) - 1 = \bar{B}_i + \bar{C}_i P \qquad (23)$$

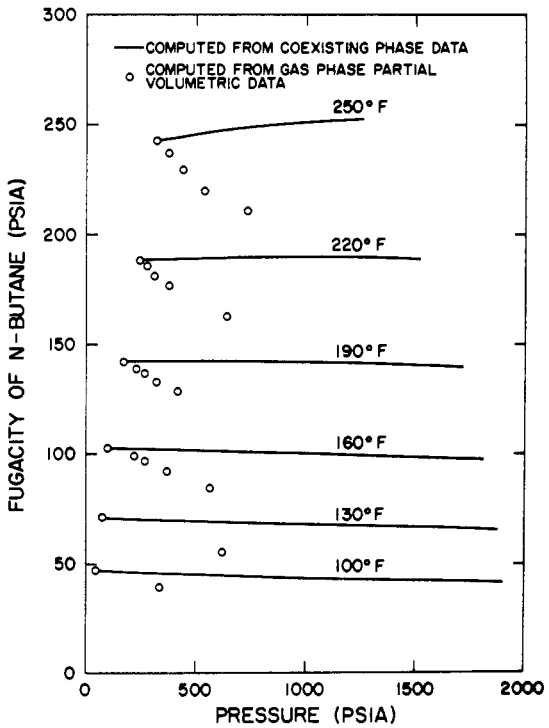

Figure 6. Fugacity of *n*-butane at saturation conditions in methane–*n*-butane system

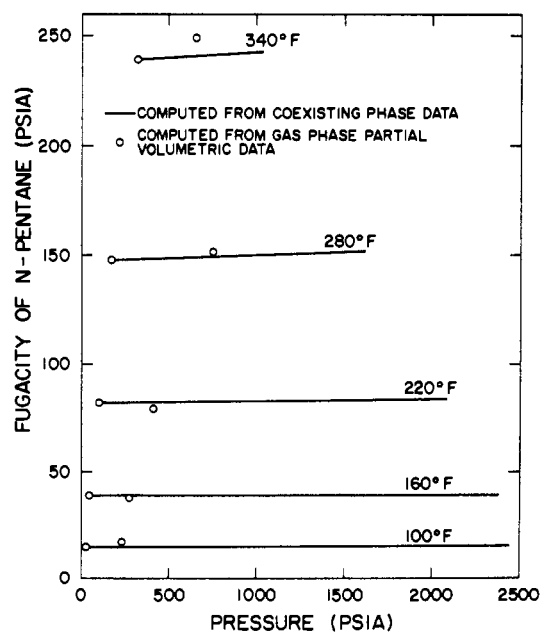

Figure 7. Fugacity of *n*-pentane at saturation conditions in methane–*n*-pentane system

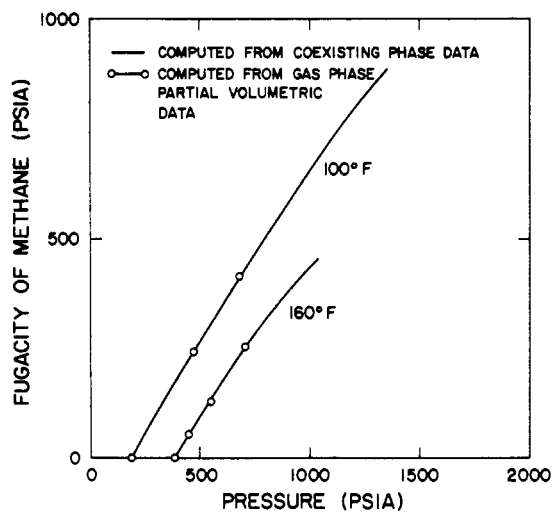

Figure 8. Fugacity of methane at saturation conditions in methane–propane system

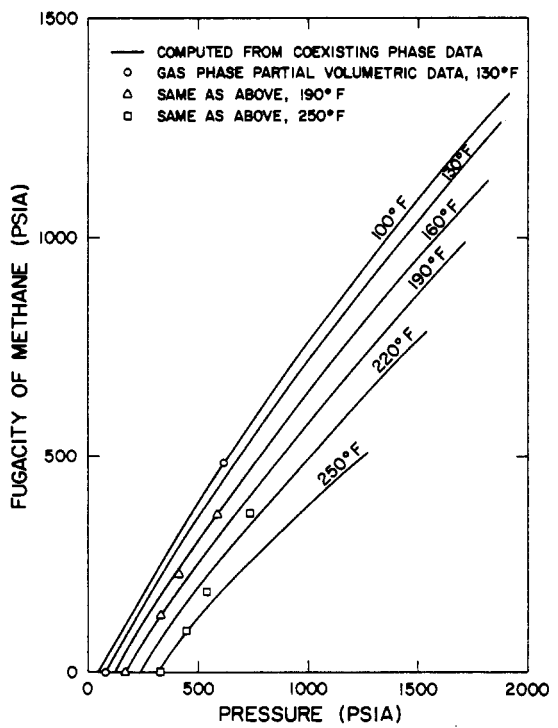

Figure 9. Fugacity of methane at saturation conditions in methane–*n*-butane system

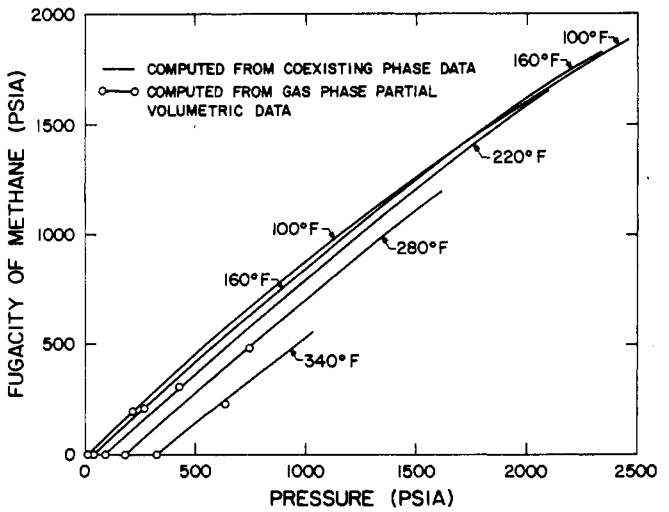

Figure 10. Fugacity of methane at saturation conditions in methane–*n*-pentane system

To integrate from point *A* to the data point on path *A–B* with the lowest pressure, the coefficient "$\bar{B}_i$" in Equation 23 was determined from second virial coefficient data, and "$\bar{C}_i$" was computed from partial volumetric data at the first data point. $\bar{B}_i$ is related to the interaction and pure component virial coefficients by the following equation:

$$\bar{B}_i = y_i[(2 - y_i)B_{ii} + y_j^2\,(2\,B_{ij} - B_{jj})]/RT \quad (24)$$

At higher pressures the coefficients in Equation 23 were determined from partial volumetric data at consecutive points on path *A–B*.

Results

The component fugacities computed for methane–propane, methane–*n*-butane, and methane–*n*-pentane are presented in Tables I–III, respectively. The fugacities of the heavier hydrocarbon in each system computed from coexisting phase data and from gas-phase partial volumetric data are shown in Figures 5–7. The fugacities of the methane in each system are shown in Figures 8–10.

The results of the two methods for computing fugacities show good agreement except for the methane–*n*-butane system. The discrepancies in this case reflect inconsistencies in the gas phase and coexisting phase data for the methane–*n*-butane systems.

The crossing of the 100° and 160°F isotherms in Figure 10 was expected. At high pressures and low temperatures, the gas phase of the methane–*n*-pentane system contains a high concentration of methane. Therefore, the fugacity of the methane in the mixture approaches the fugacity of pure methane which increases with temperature at constant pressure. The fugacity of methane at low pressures is dependent on the mole fraction of methane in the liquid phase which decreases as temperature increases at constant pressure. This causes the isotherms to cross.

Nomenclature

A, B, C, D = states on isothermal pressure composition diagram
a, b = constants in equations to compute changes in the mixture fugacity
a_i, b_i = constants in equations to compute changes in the fugacity of methane, propane, *n*-butane, or *n*-pentane
B_{ij} = second virial coefficient for a pure component when $i = j$; interaction second virial coefficient when $i \neq j$
$\bar{B}_i, \bar{C}_i$ = constants in equations for integrating gas-phase partial volumetric data
f = fugacity, $lb_F/in.^2$
ln = Naperian logarithm
N = number of moles
P = pressure, $lb_F/in.^2$
R = gas constant, $ft\text{-}lb_f/lb_m - °R$
T = temperature, °R
V = volume, ft^3
$\bar{V}_i$ = partial volume of component "*i*," ft^3/mol
x = mole fraction in liquid phase
y = mole fraction in vapor phase
1, 2, 3 = states on isothermal pressure composition diagram

Greek Letters

Δ = small change

Subscripts and Superscripts

f = properties of liquid phase
g = properties of vapor phase; saturation conditions for propane, *n*-butane, or *n*-pentane
i, j = indices
N = number of moles
P = pressure
T = temperature
0 = reference state where properties are known
1 = properties of methane
2 = properties of propane, *n*-butane, or *n*-pentane

Literature Cited

(1) Beattie, J. A., Stockmayer, W. H., *J. Chem. Phys.*, **10**, 473 (1942).
(2) Dantzler, E. M., Knobler, C. M., Windsor, M. L., *J. Phys. Chem.*, **72**, 676 (1968).
(3) Guam, R. D., MS thesis, University of California, Berkeley, Calif., 1958.
(4) Hougen, O. A., Watson, K. M., Ragatz, R. A., "Chemical Process Principles," Wiley, New York, N.Y., 1962.
(5) Leach, J. W., Chappelear, P. S., Leland, T. W., *AICHE J.*, **14** (4), 568 (1968).
(6) Lehmann, Von H., *Z. Phys. Chem. (leyzz)*, **235**, 179 (1967).
(7) McGlashan, M. L., Potter, D. J. B., *Proc. Roy. Soc. (London)*, **A267**, 478 (1962).
(8) Sage, B. H., Lacey, W. N., "Thermodynamic Properties of the Lighter Hydrocarbons and Nitrogen," American Petroleum Institute, New York, N.Y., 1950.
(9) Shim, J., Kohn, J. P., *J. Chem. Eng. Data*, **1** (1), 3 (1962).
(10) Van Ness, H. C., *Ind. Eng. Chem. Fundam.*, **10** (2), 325 (1971).

Received for review March 31, 1972. Accepted March 5, 1973.